Single-Site and Dual-Site Metallocene Ethene/Propene Copolymerizations: Experimental and Theoretical Investigations

C. Piel,[†] F. G. Karssenberg,[‡] W. Kaminsky,*[,†] and V. B. F. Mathot[‡]

Institute of Technical and Macromolecular Chemistry, University of Hamburg, Bundesstr. 45, 20146 Hamburg, Germany, and Laboratory of Polymer Technology, Eindhoven University of Technology, P.O. Box 513, 5600 MB Eindhoven, The Netherlands

Received March 18, 2005; Revised Manuscript Received June 2, 2005

ABSTRACT: Three series of ethylene−propylene copolymers are made using the catalysts (**1**) *rac*-[Me_2-Si(2-Me-4-(1-Naph)Ind)$_2$]$ZrCl_2$/MAO, (**2**) [Me_2Si(Ind)(Flu)]$ZrCl_2$/MAO, and (**3**) a 1:5 mixture of **1** and **2**, all with a broad range of (co)monomer mole fractions in the reactor and copolymers. All three series are analyzed by ^{13}C NMR, DSC, and SEC. The ^{13}C NMR spectra of the single-site series are the input of the direct peak method to determine the second-order Markov reactivity ratios of the catalysts used. The activities and reactivity ratios of the catalysts in the single-site experiments are used to model the dual-site series based on ^{13}C NMR data. The results of this modeling are used to interpretate the DSC and SEC data of the dual-site series: most of the melting peak temperatures and molar masses of the dual-site can be attributed to one of the two catalysts.

1. Introduction

Comparing conventional heterogeneous Ziegler−Natta to metallocene-based catalysis for the synthesis of polyolefins, it is surprising to see that the level of understanding of the catalytic species is almost opposite to the level of production. Even though the nature of the active species is rather incomprehensible in Ziegler−Natta catalysis, quantitatively, this way of synthesizing (co)polymers continues to dominate the market, mainly because of the lower production costs but also due to the favorable morphology and good processability of the products. On the other hand, the reaction mechanisms of homogeneous, single-site catalysts such as vanado-, zirco-, titano-, and hafnocenes and constrained geometry catalysts (CGC's) are nowadays well understood. Nevertheless, the polyolefins made by single-site catalysts only possess a relatively small part of the world market. Because of the narrow distributions of molar masses (MMD), which in the case of polyethylenes (PE's) is unfavorable for the processing, modulations of the molecular architectures have become necessary. This was reached via two main routes: introduction of long-chain branches (LCB's) in polyethylenes like low-density PE (LDPE) and (in-situ) blending. Obviously, the target is to combine the best of both, the good processability and the good mechanical properties.

Long-chain branching in metallocene-catalyzed polymers has been the subject of intense research since the first patents were published in the mid-1990s.[1,2] The first single-site catalyst reported to produce long-chain branched polyethylene was the CGC.[2,3] LCB in polyethylene has several benefits relating to the polymer processability[4−7] since it affects the melt viscosity, temperature dependence of viscosity, melt elasticity, shear thinning, and extension thickening.

An opportunity to tune high density PE (HDPE) is to produce blends. Apart from the MMD and comonomer distribution that a certain catalyst produces in polymerization in one reactor, two or more cascaded reactors with different polymerization conditions increase the freedom to tailor polymer properties by in-situ blending of two or more structurally different polyethylenes. The bimodal process technique has been mostly used to improve processability and the mechanical properties of HDPE.[8] Bimodal polyethylene consists of two or more polymer fractions which usually differ from each other with respect to molar mass and branching (comonomer) content, and in fact, such a grade leads to intermolecular heterogeneity.[9−12] In a bimodal process, the catalyst is fed into the first reactor where the first polymer fraction is produced. After that the polymer fraction is transferred into the second reactor for production of the second polymer fraction. In some of the bimodal processes the reactor may also be operated in parallel mode.

Traditionally, bimodal polyethylene resins are produced with Ziegler−Natta type catalyst, but for specialty grades (e.g., bimodal linear low density PE) the use of metallocene catalysts is slowly increasing.[8] The application areas of bimodal polyethylene are the same as for corresponding monomodal resins. However, optimizations of product−property combinations, such as the stiffness−impact balance, can result in products with higher performance. For example, without polyethylenes of controlled bimodal MMD and comonomer incorporation, development of HDPE pipe materials with better environmental stress crack(ing) resistance (ESCR) and higher pressure classification would not have been possible.[8,10,12,13]

A promising way to understand and by that to tailor the microstructure and molar mass distribution of polyolefins is the use of mixed metallocene systems, since mixtures of well-defined single-site catalysts are good model systems. Over the past years, the number of publications on binary, dual-site, or mixed catalysts for the production of polyethylene,[14−25] polypropylene,[26−29] and ethene/α-olefin copolymers[13−18,30−33] has therefore grown tremendously.

In this study three series of ethylene−propylene copolymers were produced using the catalyst precursors

[†] University of Hamburg.
[‡] Eindhoven University of Technology.
* To whom correspondence should be addressed: Fax +49 40 42838 6008; e-mail kaminsky@chemie.uni-hamburg.de.

10.1021/ma0505732 CCC: $30.25
Published on Web 07/15/2005

(**1**) *rac*-[Me_2Si(2-Me-4-(1-Naph)Ind)$_2$]$ZrCl_2$, (**2**) [Me_2Si(Ind)(Flu)]$ZrCl_2$, and (**3**) a 1:5 mixture of **1** and **2**, all with a broad range of (co)monomer mole fractions in the reactor and copolymers. Catalyst **1** produces rather random ethylene−propylene copolymers[34] with a high affinity to incorporate propene whereas alternating copolymers with low amounts of propene are synthesized by catalyst **2**.[35] The aim of this study is to create a better understanding of dual-site catalysis with the help of single-site results. The activities of the single-site series are used to calculate the contributions of the two catalysts in the dual-site experiments, and carbon-13 nuclear magnetic resonance (^{13}C NMR) data are used for the modeling of the propene incorporation in the copolymers and the reactivity ratios of the three catalyst systems. On the basis of this modeling, the results of differential scanning calorimetry (DSC) and size exclusion chromatography (SEC) measurements are interpreted.

Some of the published studies on ethene/α-olefin copolymers also investigate the possible interactions between two metallocenes, focusing on ligand exchange[30] as well as on chain transfer from site to site in solution[30−32] or on supported systems.[33] In this study though, ligand exchange is excluded because of the use of bridged metallocenes. Also, the phenomenon of chain transfer is debarred, as the catalyst concentrations were kept very low to minimize the probability to incorporate a vinyl-terminated polymer chain. For this reason we assume that each chain is built up by only one unchanging site. As will be shown, the molar mass distributions of the copolymers do not indicate otherwise.

The catalyst, the polymerization conditions, and the polymerization reactor operating conditions are all significant for the comonomer incorporation. In a batch polymerization the concentrations of the (co)monomer decrease as the polymerization proceeds, but not to the same extent. In a semibatch polymerization only the monomer concentration is constant. In the continuous stirred tank reactor (CSTR) system monomer and comonomer concentrations are both constant after the steady-state conditions are achieved. Here the semibatch process was used as only ethene was fed during the reaction; therefore, the polymerization time has an influence on the comonomer concentration and incorporation. The propene conversion was kept very low in order to achieve intermolecular homogeneous fractions for each polymer.

2. Experimental Details

2.1. General Comments. All operations were performed under a dry argon atmosphere using standard Schlenk techniques.

2.2. Chemicals. The solvent toluene and the monomers ethene (Messer Griesheim) and propene (Linde) were purified passing through two columns with a 4 Å molecular sieve and BASF copper catalyst R3-11. Methylaluminoxane (MAO, Crompton) solution was filtered, the toluene and trimethylaluminum (TMA) were removed in vacuo, and MAO was stored as a solid. Fresh prepared solutions in dry toluene were used for polymerizations.

2.3. Catalysts. The catalysts used are (**1**) *rac*-[Me_2Si(2-Me-4-(1-Naph)Ind)$_2$]$ZrCl_2$/MAO, (**2**) [Me_2Si(Ind)(Flu)]$ZrCl_2$/MAO, and (**3**) a mixture of the catalysts **1** and **2**. Catalyst precursor **1** was purchased from Boulder Scientific Inc. and precursor **2** from MCAT GmbH, Germany (see Figure 1). Both were stored under an argon atmosphere, and fresh solutions in dry toluene were prepared prior use.

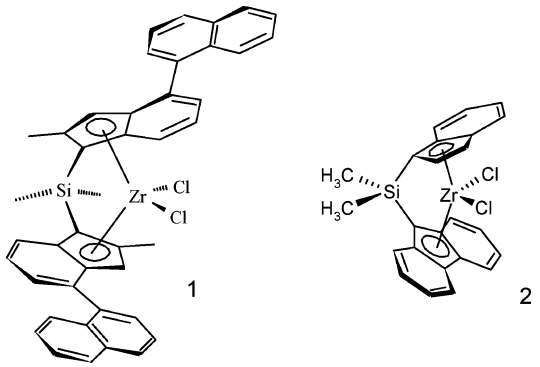

Figure 1. Catalyst precursors: **1**, *rac*-[Me_2Si(2-Me-4-(1-Naph)Ind)$_2$]$ZrCl_2$; **2**, [Me_2Si(Ind)(Flu)]$ZrCl_2$.

2.4. Polymerizations. Polymerizations were carried out in 400 mL of toluene at 30 °C in a 1 L Büchi glass reactor equipped with a magnetical stirrer. The propene and ethene pressure for every run were set, and the pressure was kept constant during the polymerization; ethene was fed constantly (semibatch process). The monomer concentrations were calculated using literature data.[36] The total monomer concentration and propene feed in the reactor are listed in Table 1. The polymerizations were started by injection of the metallocene complex or complex mixture in toluene to the propene and ethene saturated toluene/MAO (400 mg) solution. The catalyst precursor amount for the single-site series was 5×10^{-8} mol for catalyst **1** and 5×10^{-7} mol for catalyst **2**. For the dual-site series a mixture of catalysts **1** and **2** was used with a molar ratio of 1:5 and a total catalyst amount of 1.5×10^{-7} mol per polymerization. The ratio of the activities of catalysts **1** and **2** for ethene reactor feeds around 50 mol % is 5:1, and so to obtain balanced bimodal copolymers the ratio 1:5 was applied. After a short polymerization period (propene conversion < 5%) the reaction was stopped by addition of 1 mL of ethanol. The polymer solution was stirred overnight in a ethanol/HCl/water solution and filtered followed by washing with plenty of ethanol and drying of the polymer in vacuo at 60 °C overnight.

2.5. Polymer Analysis. The ^{13}C NMR samples were prepared by the dissolution of the polymers (10 mass %) in a mixture of 1,2,4-trichlorobenzene and 1,1,2,2-tetrachloro-1,2-dideuterioethane and were measured at 100 °C, pulse angle 30°, delay time 5 s, 1024 scans on a Bruker 400-MHz NMR spectrometer using the waltz16 decoupling method and referenced against $C_2D_2Cl_4$. The experimental propylene content in the copolymers was determined using the Randall method.[37]

The thermal behavior of the polymers was measured using a Mettler-Toledo DSC 821e, in the temperature range from −100 to 200 °C with a heating rate of 20 K min^{-1}. To determine the melting temperatures, the second heating run was used.

SEC was carried out with a Waters GPCV 2000 Alliance system equipped with a refractive index detector, viscosimetric detector, and a set of three columns, Styragel type (HT6, HT5, HT3). 1,2,4-Trichlorobenzene was used as solvent. The analyses were performed at 140 °C and 1.0 mL min^{-1} flow rate. The system was calibrated with narrow molar mass distribution polystyrene standards and their Mark−Houwink constants using the universal method. The sample concentration was 1 mg mL^{-1}, and 2,6-di-*tert*-butyl-4-methylphenol was used as thermostabilizer. The molar masses were calculated using the refractive index signal and literature constants for polyethylene ($K = 0.0406$ mL g^{-1}, $a = 0.725$) and corrected for propylene content using the method by Scholte et al.[38]

3. Results and Discussion

3.1. Activities and Contributions. The activities of all three series and the contribution of catalyst **2** to the bimodal polymers are listed in Table 1 and shown in Figure 2. For all copolymerizations catalyst **1** gives higher activities with a maximum for pure polyethylene of about 800 $t_{polymer}$ mol_{Zr}^{-1} h^{-1} $mol_{monomer}^{-1}$ L. Catalyst

Table 1. Total Monomer Concentrations, Propene Reactor Feed, Activities of the Catalysts, and Contribution of Catalyst 2 to the Dual-Site Polymers

	catalyst **1**		catalyst **2**		dual-site series[a]		
c_{tot}[b]	C_3 feed[c]	activity[d]	C_3 feed[c]	activity[d]	C_3 feed[c]	activity[d]	contrib[e]
0.6	0	800	0	19	0	155	0.11
0.6	11	700	11	18	11	160	0.12
0.8	21	550	21	20	21	98	0.16
0.8	31	400	31	22	31	76	0.22
1.0	45	210	39	22	41	55	0.35
1.0	50	200	50	20	50	18	0.34
1.0	60	130	60	17	60	37	0.41
1.0	70	80	70	20	70	27	0.57
1.0	80	60	80	25	80	29	0.68
1.0	90	40	90	20	90	18	0.72
1.0	95	30	95	16	95	2	0.73
2.0	98	25	98	13	98	3	0.73
2.0	99	16	99	8	99	3	0.72
2.0	100	11	100	4	100	2	0.65

[a] 1:5 mixture of catalysts **1** and **2**. [b] Total monomer concentration [mol L^{-1}]. [c] Propene feed in the reactor [mol %]. [d] [$t_{polymer}$ mol_{Zr}^{-1} h^{-1} $mol_{monomer}^{-1}$ L]. [e] Contribution of catalyst **2** to the bimodal polymers = 5 × $activity_{cat.2}$/($activity_{cat.1}$ + 5 × $activity_{cat.2}$).

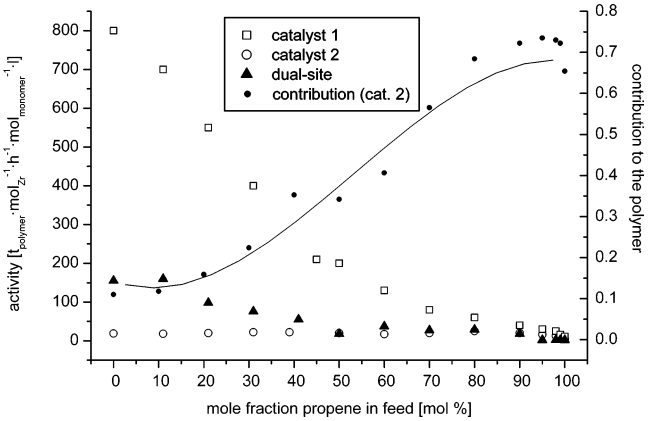

Figure 2. Catalyst activities and the contribution of catalyst **2** to the bimodal polymers. The contribution line is added for guidance to the eye.

2 is much less active for copolymerizations with high ethylene content, but for polypropylene and copolymers with high propylene content the activities are rather close to the ones of catalyst **1**. Most of the activities of the dual-site series are in between the ones of the single-site experiments.

The contribution of catalyst **2** to the dual-site experiments is calculated from the single-site activities and the catalyst molar ratio of 1:5. Because of the nonparallel course of the activities of the two catalysts, the contribution of catalyst **2** is not only dependent on the catalysts molar ratio but also on the mole fraction of propene in feed. In the reactor feed range 0−60 mol % the activity of catalyst **2** is more than 5 times lower than the activity of catalyst **1**, and therefore the contribution of catalyst **2** to the dual-site experiments is smaller than 50% and vice versa in the reactor feed range 70−100 mol %.

3.2. Modeling of NMR Data and Comonomer Incorporation. The recently published direct peak method (DPM)[39] enables the modeling of comonomer incorporation and reactivity ratios of single-site catalysts based on the ^{13}C NMR data of series of homogeneous ethylene−1-alkene copolymers. This DPM has been successfully applied to series of metallocene-catalyzed ethylene−propylene copolymers before[40,41] and is also used here to model the single-site experiments. As will be shown, the reactivity ratios of the single-site catalysts can be used to describe the propene incorporation of the copolymers in the dual-site series.

Table 2 presents reactor feed and propene incorporation for the two single-site series and the second-order Markov reactivity ratios of the two catalysts. As mentioned before, the experimental feed was calculated from the (co)monomer pressures and the experimental propylene incorporation from the ^{13}C NMR data using the Randall method. The experimental feed and the ^{13}C NMR spectra have been used as input of the DPM for the second-order Markov modeling of the reactor feed, the propene incorporation, and the reactivity ratios. The use of second-order Markov is justified, since first-order Markov statistics do not satisfy the 99.5% reliability condition.[41] For each of the two single-site series, the total number of equations fitted in the model is equal to 108, (8 + 1) × 12, namely 8 NMR regions and 1 feed for all 12 copolymers. The number of variables is 28: per copolymer 1 reactor feed and 1 scaling factor plus 4 reactivity ratios. The total number of degrees of freedom is 108 − 28 = 80. With χ^2 values of 40.3 and 47.8 for catalyst **1** and **2**, respectively, all results reflect a reliability >99.8%.

The experimental and modeled results presented in Table 2 are depicted in Figure 3. At high propene concentrations in the reactor, the difference between the two catalysts is very pronounced: catalyst **1** easily incorporates comonomer units while for catalyst **2** it is hardly possible to insert more than about 50 mol % of propene even at ethene−propene ratios in the feed of [P] = 99 mol %. In a growing chain, the addition of new monomer and comonomer units is mainly determined by the reactivity ratios of the active site(s) of the catalyst. The reactivity ratios are calculated by $r_{hij} = k_{hii}/k_{hij}$ with h, i, j element of {E, P} and k the reaction rate constants and are described in detail in ref 39. The square root of the product of the 4 reactivity ratios represents the classical "$r_E r_P$" value which reveals the character of the catalyst.[39] Here the values 2.02 and 0.03 demonstrate that catalyst **1** produces rather random and catalyst **2** alternating copolymers.

In the DPM for single-site copolymers, the reactivity ratios and reactor feeds determine the ^{13}C NMR spectra via propagation probabilities and diad fractions, and the theoretical spectra are multiplied by scaling factors to enable the comparison with experimental ones (see Figure 4a). The modeling of dual-site experiments now is rather straightforward since the copolymerization

Table 2. Experimental and Modeled Propene Feed and Propene Incorporation of the Single-Site Series and Reactivity Ratios of the Two Catalysts

catalyst **1**				catalyst **2**			
feed $C_3/(C_2 + C_3)$[a]		C_3 incorporation[b]		feed $C_3/(C_2 + C_3)$[a]		C_3 incorporation[b]	
exp	model	exp	model	exp	model	exp	model
0	0.0	0.0	0.0	0	0.0	0.0	0.0
11	10.7	0.4	2.1	11	9.3	1.2	1.4
21	17.8	3.6	4.0	21	22.2	3.9	3.8
31	24.9	5.2	6.2	31	30.9	5.9	5.9
45	44.0	15.7	15.1	39	40.8	9.3	8.7
50	53.8	23.2	22.3	50	55.3	14.8	14.4
60	65.5	34.9	34.7	60	61.3	17.7	17.5
70	74.2	46.8	48.1	70	67.1	21.0	21.0
80	85.1	68.6	69.5	80	77.8	28.8	29.1
90	91.1	81.3	82.5	90	87.9	38.6	39.2
95	95.5	90.0	91.6	95	94.5	46.8	47.4
98	97.9	95.0	96.4	98	96.5	49.7	50.4
99	98.8	95.7	98.3	99	96.3	50.0	50.8
100	100.0	100.0	100.0	100	100.0	100.0	100.0
r_{EEP}		5.46 (±6.2%)		r_{EEP}		7.23 (±4.7%)	
r_{EPE}		0.37 (±5.4%)		r_{EPE}		0.006 (±10.0%)	
r_{PEP}		3.43 (±6.1%)		r_{PEP}		3.29 (±5.5%)	
r_{PPE}		0.59 (±4.2%)		r_{PPE}		0.007 (±51.4%)	
"$r_E r_P$"[c]		2.02 (±11.2%)		"$r_E r_P$"[c]		0.03 (±37.2%)	
no. of equations		108		no. of equations		108	
no. of variables		28		no. of variables		28	
no. of dof		80		no. of dof		80	
χ^2		40.3		χ^2		47.8	
reliability		99.99%		reliability		99.84%	

[a] Mole fraction propene in reactor feed [mol %]. [b] Mole fraction propylene in copolymer [mol %]. [c] See text and ref 39; dof = degrees of freedom.

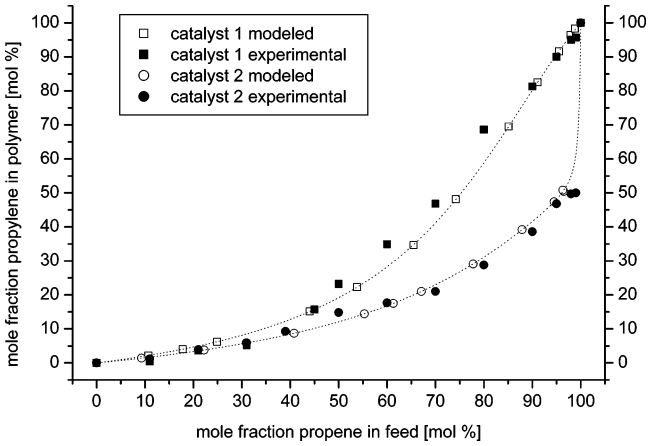

Figure 3. Experimental and modeled propene incorporation of the single-site series.

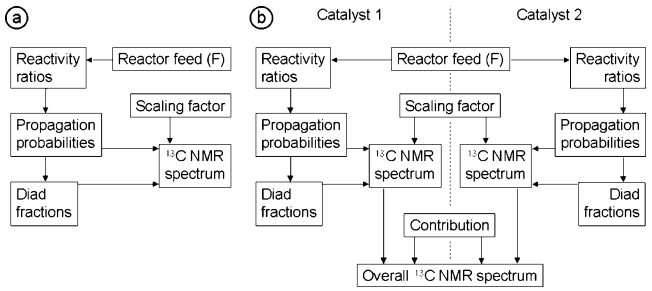

Figure 4. Schematics of the second-order Markov direct peak method for the modeling of (a) single-site and (b) dual-site copolymers.

reaction at two sites is a combination of two single-site reactions. In the dual-site reactions described here, two catalysts operate independently and simultaneously, creating exactly the same copolymers as in single-site experiments. Therefore, the DPM, developed for the modeling of single-site catalysts, only needs minor changes to be able to also model dual-site catalysts. In the DPM for dual-site copolymers (Figure 4b), two ^{13}C NMR spectra are calculated on the basis of two different sets of reactivity ratios, and these spectra both contribute to the overall spectrum.

Table 3. Experimental and Modeled Propene Feed and Propene Incorporation of the Dual-Site Series

feed $C_3/(C_2 + C_3)$[a]		C_3 incorporation[b]			
				model per catalyst	
exp	model	exp	model overall	cat. **1**	cat. **2**
0	0.0	0.0	0.0	0.0	0.0
11	9.0	0.7	1.8	1.8	1.3
21	18.6	3.0	4.1	4.3	3.1
31	29.6	7.3	7.5	8.0	5.5
41	39.9	11.6	11.5	12.7	8.4
50	48.1	14.9	15.4	17.8	11.3
60	61.9	24.8	24.5	30.4	17.8
70	73.4	33.8	34.9	46.6	25.5
80	83.7	46.0	46.7	66.5	34.7
90	89.6	52.5	53.7	83.0	38.8
95	95.5	65.3	62.6	94.8	50.5
98	98.4	72.5	69.7	97.2	56.8
99	99.4	79.9	77.6	99.0	67.6
100	100.0	100.0	100.0	100.0	100.0

[a] Mole fraction propene in reactor feed [mol %]. [b] Mole fraction propylene in copolymer [mol %].

An overview of the experimental and modeled reactor feed and propene incorporation of the dual-site experiments is shown in Table 3. Analogously to the single-site experiments, the experimental feed is calculated from the gas pressures and the experimental propene incorporation from the ^{13}C NMR data (Randall method). The modeled data in Table 3 are the results of the DPM for the modeling of dual-site copolymers using the contributions of the two catalysts (see Table 1) and the second-order Markov reactivity ratios (see Table 2). The overall propylene content is calculated from the overall ^{13}C NMR spectrum, and the propylene content splitted

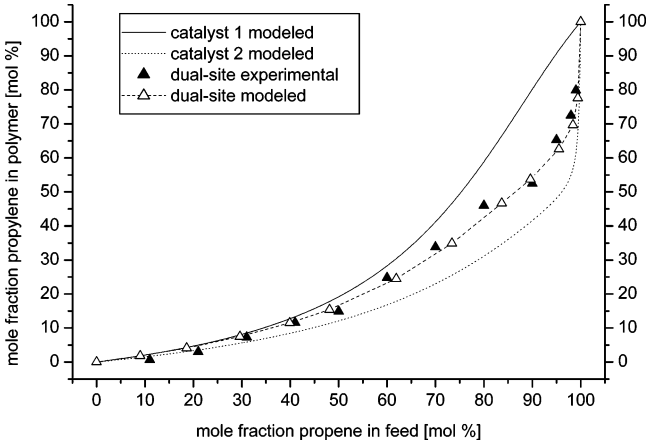

Figure 5. Experimental and modeled propene incorporation of the dual-site series. Outer lines represent the theoretical single-site behavior of catalysts **1** and **2**.

Table 4. Reactivity Ratios of the Catalysts 1 and 2 Obtained from the Single-Site and Dual-Site Series

	catalyst **1**		catalyst **2**	
	single-site[a]	dual-site	single-site[a]	dual-site
r_{EEP}	5.46 (±6.2%)	5.71	7.23 (±4.7%)	8.83
r_{EPE}	0.37 (±5.4%)	0.25	0.006 (±10.0%)	0.005
r_{PEP}	3.43 (±6.1%)	2.57	3.29 (±5.5%)	4.67
r_{PPE}	0.59 (±4.2%)	0.86	0.007 (±51.4%)	0.05
"$r_E r_P$"	2.02 (±11.2%)	1.78	0.03 (±37.2%)	0.10
no. of equations	108	108	108	108
no. of variables	28	32	28	32
no. of dof	80	76	80	76
χ^2	40.3	63.5	47.8	63.5
reliability	99.99%	84.63%	99.84%	84.63%

[a] See Table 2.

per catalyst originates from the ^{13}C NMR spectra before applying the contributions. Note that for catalyst **2** the modeled propylene contents at 98 and 99 mol % propene exceed the experimental limitation of 50 mol %.

The experimental and modeled results of the dual-site series presented in Table 3 are plotted in Figure 5 together with the second-order Markov lines of the single-site series. This plot clearly shows the effect of the contribution to the dual-site results. For low propene feeds in the reactor, the contribution of catalyst **2** is low; therefore, most of the copolymer chains are produced by catalyst **1**, but with increasing propene feed the propylene contents of the dual-site copolymers move away from the second-order Markov line of catalyst **1** toward the one of catalyst **2**.

As an additional step, the reactivity ratios of the two metallocenes can also be estimated from the dual-site results. Therefore, the modeling can be repeated without making use of the reactivity ratios found by the DPM for the single-site series. In this case, the reactivity ratios of the two catalysts are set as variables and determined via χ^2 minimalization of the overall theoretical and experimental ^{13}C NMR spectra of the series of copolymers. The activities of the two catalysts in the single-site experiments and the molar ratio 1:5 are still used to calculate the contributions (see Table 1). Compared to the modeling of the single-site series, the number of equations remains the same (108) and the number of variables increases to 32 (8 reactivity ratios instead of 4). The results are listed in Table 4 in addition to the values found by the modeling of the single-site series.

Table 5. Melting Points and Weight-Average Molar Masses of the Single-Site and Dual-Site Made Copolymers

a. Single-Site Made Copolymers[a]

catalyst **1**			catalyst **2**		
C_3 incorp[b]	T_m [°C]	M_w [kg mol^{-1}]	C_3 incorp[b]	T_m [°C]	M_w [kg mol^{-1}]
0.0	131.4	345	0.0	138.3	341
2.1	110.1	218	1.4	129.9	228
4.0	114.6	219	3.8	112.8	125
6.2	107.1	290	5.9	102.5	98
15.1	59.7	162	8.7	89.6	68
22.3	44.7	144	14.4	65.4	49
34.7		130	17.5	41.3	43
48.1		130	21.0	20.1	37
69.5		135	29.1		30
82.5	83.1	185	39.2		25
91.6	117.2	281	47.4		23
96.4	139.6	469	50.4		23
98.3	142.7	563	50.8		23
100.0	152.5	888	100.0		43

b. Dual-Site Made Copolymers

C_3 incorporation[b]			T_m [°C]		M_w [kg mol^{-1}]	
overall	catalyst **1**	catalyst **2**	peak 1	peak 2	mass 1	mass 2
0.0	0.0	0.0	137.9		331	
1.8	1.8	1.3	130.3		338	
4.1	4.3	3.1	115.5		292	
7.5	8.0	5.5	95.3		250	
11.5	12.7	8.4	52.7	88.0	137	
15.4	17.8	11.3	80.4		82	
24.5	30.4	17.8	62.5		78	
34.9	46.6	25.5			71	
46.7	66.5	34.7			83	
53.7	83.0	38.8	105.6		27	230
62.6	94.8	50.5	133.5		22	471
69.7	97.2	56.8	145.0		24	592
77.6	99.0	67.6	150.0		25	649
100.0	100.0	100.0	152.7		41	910

[a] Polydispersity of all polymers is close to 2. [b] Modeled mole fraction propylene in copolymer [mol %].

Even though the reactivity ratios found by the modeling of the dual-site series are not as precise as the ones modeled by the single-site series (see Table 4), clearly these results are a good estimate and show great resemblance. The trends that $r_{EEP} > r_{PEP}$ and $r_{EPE} < r_{PPE}$[41,42] are also found. These results prove that, in the case the catalysts act independently, overall ^{13}C NMR spectra of dual-site copolymers can be split up into contributions of the two catalysts used.

3.3. Melting Temperatures and Molar Masses. Table 5a shows an overview of the melting peak temperatures of the polymers of the two single-site series. The melting temperatures of the single-site made copolymers with low propylene content are almost independent of the catalyst type. From recent Monte Carlo simulations[43] on crystallization and melting of copolymers with different distributions of the comonomer units in the chain, it was expected that the influence of increasing propylene content would be slightly higher for catalyst **2** than for catalyst **1**. The latter is producing more random copolymers, so longer ethylene sequences also exist for higher propene incorporation. With catalyst **2** alternating sequences in the copolymers are synthesized, so longer ethylene sequences disappear faster with increasing comonomer

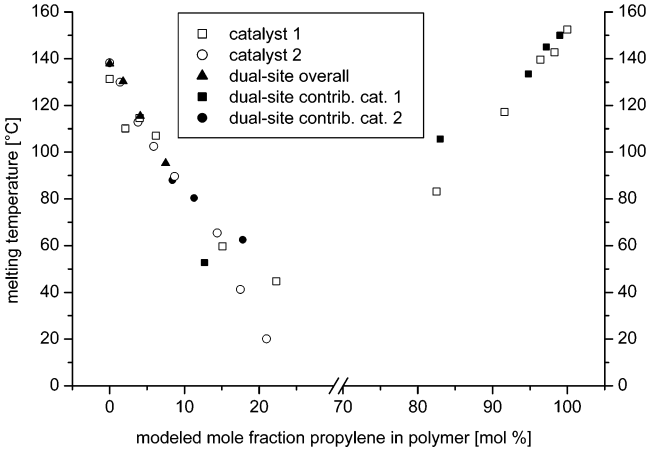

Figure 6. Melting temperatures vs modeled propene incorporation of the dual-site series.

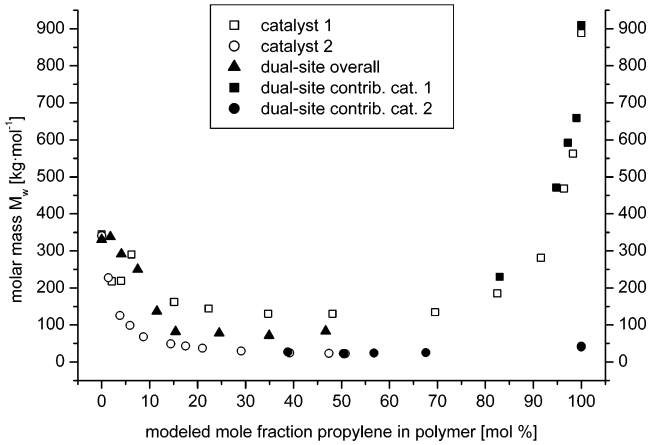

Figure 7. Weight-average molar masses vs modeled propene incorporation of dual-site series.

content. In combination with the decreasing molar masses of catalyst **2** made fractions, a slightly smaller influence of increasing propylene content on catalyst **1** compared to catalyst **2** was expected, but this is not observed indisputably.

For copolymers produced at high propene reactor feeds, the influence of catalyst type on the melting behavior is much more pronounced. If the propylene mole fraction is more than 80 mol %, catalyst **1** is producing partly crystalline copolymers and catalyst **2** only incorporates propene up to 50 mol % and reflects no propylene crystallinity. These results are in line with products previously made by these catalysts.[34,35] While catalyst **1** is producing highly isotactic polypropylene with a melting point over 150 °C, catalyst **2** made polypropylene is rather atactic (hemiisotactic tendence). Therefore, no melting point is observed for this polymer.

The data of the dual-site series are summarized in Table 5b, while Figure 6 shows the melting points of all three series vs the propylene content in the polymers. A comparison of the single-site series and the dual-site series allows an assignment of some data to catalyst **1** or **2**. The observed melting peaks of the first four polymers of the dual-site series can originate either from catalyst **1** or catalyst **2**; the differences in this area are too small to indisputably assign these peaks to one of the catalysts. Therefore, in Figure 6 these points are plotted vs the overall propylene content. On the basis of the modeled propene incorporations, the double melting peak at 88.0 and 52.7 °C can be assigned to catalyst **2** and catalyst **1**, respectively. The melting temperatures of 62.5 and 80.4 °C can only be originating from catalyst **2**; at this propylene content the polymers made by catalyst **1** have already lower or no melting points. Copolymers with high propylene content and crystallinity are not produced by catalyst **2**, so the last four melting peaks in this series can only be originating from catalyst **1**.

As shown in Table 5a, the molar masses of the polymers synthesized with catalyst **1** are much higher than the ones made by catalyst **2**. All molar mass distributions are at about 2 as expected for single-site experiments. Catalyst **1** shows a minimum in the molar masses. The masses are high for polyethylene and copolymers with low propylene content and high for polypropylene and copolymers with high propylene content. In between the molar masses are lower; this was also observed in previous studies.[34] Catalyst **2** shows a decrease of the molar masses with increasing comonomer content. The highest mass was reached for polyethylene and the lowest for copolymers with higher propylene content. A general trend in these series is that the polymers made by catalyst **1** have higher molar masses than those made by catalyst **2**.

The SEC results of the dual-site series are given in Table 5b. A separation of the molar masses of the samples with an overall propylene content of less than 50 mol % was not possible. Because of the mixture of a high molar mass fraction made by catalyst **1** and a lower molar mass fraction made by catalyst **2**, the nonseparated average molar masses are in between those of the single-site experiments. The results are plotted in Figure 7. The five samples with the highest overall comonomer content can be separated, and this leads to two weight-average molar masses M_w. The shorter chains are originating from catalyst **2** and the longer chains from catalyst **1**. For these samples the MMD of each fraction was close to 2, and no peak shoulders were observed. Especially the bimodal polypropylene shows two molar masses that are very close to those of the single-site experiments and in the case of catalyst **2** almost the same.

For the last two bimodal copolymers in this series the modeling predicts a propylene incorporation of more that 50 mol % for catalyst **2** (see section 3.2), which conflicts with the single-site experiments of this catalyst. Although in this case the modeled propylene content is too high, the measured molar masses are attributed to the proper fraction.

4. Conclusions

The second-order Markov reactivity ratios of the metallocene catalysts have been successfully modeled using the direct peak method,[39,40] resulting in r_{EEP} = 5.46 (±6.2%), r_{EPE} = 0.37 (±5.4%), r_{PEP} = 3.43 (±6.1%), and r_{PPE} = 0.59 (±4.2%) for *rac*-[Me_2Si(2-Me-4-(1-Naph)-Ind)$_2$]$ZrCl_2$/MAO (catalyst **1**) and r_{EEP} = 7.23 (±4.7%), r_{EPE} = 0.006 (±10.0%), r_{PEP} = 3.29 (±5.5%), and r_{PPE} = 0.007 (±51.4%) for [Me_2Si(Ind)(Flu)]$ZrCl_2$/MAO (catalyst **2**). The use of second-order Markov statistics is justified since first-order Markov statistics do not satisfy the condition of a 99.5% reliability of the modeling.[41] The (product of the) reactivity ratios show that in ethene/propene copolymerizations catalyst **1** produces rather random copolymers with a high affinity to incorporate propene whereas catalyst **2** synthesizes

alternating copolymers with low amounts of propylene; these observations are in line with previous work on these catalysts[34,35] which shows good reproducibility of the results.

Comparing the activities of the two metallocene catalysts used, for all copolymerizations catalyst **1** gives higher values with a maximum for pure polyethylene of about 800 $t_{polymer}$ mol_{Zr}^{-1} h^{-1} $mol_{monomer}^{-1}$ L. Catalyst **2** is much less active for copolymerizations with high ethylene content, but for polypropylene and copolymers with high propylene content the activities of the two catalysts are comparable.

The activities of the single-site experiments in combination with the 1:5 catalyst's molar ratio for the dual-site copolymerizations can be used to calculate the contributions of the two active sites to the bimodal polymers. These contributions together with the second-order Markov reactivities of the single-site series enable the modeling of the dual-site experiments based on the fitting of the ^{13}C NMR spectra. As a result, the overall propylene contents of the bimodal polymers can be splitted up into the contents of the two polymer fractions belonging to the two catalysts.

On the basis of these two propylene contents of the bimodal polymers the results of DSC and SEC can be interpretated in a much better way. Melting temperatures of ethylene-type and propylene-type crystallinity as well as molar masses have been attributed to one of the two catalysts.

Finally, the second-order Markov reactivity ratios of the two catalysts can also be calculated by modeling of the ^{13}C NMR spectra of the dual-site experiments by only making use of the contributions. Even though the results of this modeling are not as accurate as the reactivity ratios obtained from applying the DPM to single-site series, the rough characteristics of the two catalysts are detected and the ratios are well estimated.

References and Notes

(1) Brant, P.; Canich, J. A. M.; Dias, A. J.; Bamberger, R. L.; Licciardi, G. F.; Henrichs, P. M. Int. Pat. Appl. WO 94/07930, 1994.
(2) Lai, S.-Y.; Wilson, J. R.; Knight, G. W.; Stevens, J. C.; Chum, P.-W. S. U.S. Patent 5,272,236, 1993.
(3) Kim, Y. S.; Chung, C. I.; Lai, S. Y.; Hyun, K. S. *J. Appl. Polym. Sci.* **1996**, *59*, 125.
(4) Dealy, J. M.; Wissbrun, K. F. *Melt Rheology and its Role in Plastics Processing: Theory and Applications*; Van Nostrand Reinhold: New York, 1990; p 665.
(5) Macosko, C. W. *Rheology: Principles, Measurements, and Applications*; Wiley-VCH: New York, 1994; p 550.
(6) Laun, H. M. *Prog. Colloid Polym. Sci.* **1987**, *75*, 111.
(7) Gahleitner, M. *Prog. Polym. Sci.* **2001**, *26*, 895.
(8) Knuuttila, H.; Lehtinen, A.; Nummila-Pakarinen, A. *Adv. Polym. Sci.* **2004**, *169*, 13.
(9) Knuuttila, H.; Lehtinen, A.; Salminen, H. In *Metallocene-Based Polyolefins*; Scheirs, J., Kaminsky, W., Eds.; Wiley: Chichester, 2000; pp 364−378.
(10) Scheirs, J.; Böhm, L. L.; Boot, J. C.; Leevers, P. S. *Trends Polym. Sci.* **1996**, *4*, 408.
(11) Mathot, V. B. F.; Pijpers, T. F. J. *Polym. Bull. (Berlin)* **1984**, *11*, 297.
(12) Mathot, V. B. F. In *Calorimetry and Thermal Analysis of Polymers*; Mathot, V. B. F., Ed.; Hanser Publishers: München, 1994; Chapter 9.
(13) Böhm, L. L.; Enderle, H. F.; Fleissner, M. *Adv. Mater.* **1992**, *4*, 234.
(14) Heiland, K.; Kaminsky, W. *Makromol. Chem.* **1992**, *193*, 601.
(15) Chu, K.-J.; Soares, J. B. P.; Penlidis, A. *Macromol. Chem. Phys.* **2000**, *201*, 340.
(16) Soares, J. B. P.; Kim, J. D. *J. Polym. Sci., Part A: Polym. Chem.* **2000**, *38*, 1408.
(17) Kim, J. D.; Soares, J. B. P. *J. Polym. Sci., Part A: Polym. Chem.* **2000**, *38*, 1417.
(18) Kim, J. D.; Soares, J. B. P. *J. Polym. Sci., Part A: Polym. Chem.* **2000**, *38*, 1427.
(19) Ahlers, A.; Kaminsky, W. *Makromol. Chem., Rapid Commun.* **1998**, *9*, 457.
(20) D'Agnillo, L.; Soares, J. B. P.; Penlidis, A. *J. Polym. Sci., Part A: Polym. Chem.* **1998**, *36*, 831.
(21) Han, T. K.; Choi, H. K.; Jeung, D. W.; Ko, Y. S.; Woo, S. I. *Macromol. Chem. Phys.* **1995**, *196*, 2637.
(22) Kim, J. D.; Soares, J. B. P.; Rempel, G. L. *J. Polym. Sci., Part A: Polym. Chem.* **1999**, *37*, 331.
(23) Liu, J.; Rytter, E. *Macromol. Rapid Commun.* **2001**, *22*, 952.
(24) Beigzadeh, D.; Soares, J. B. P.; Duever, T. A. *Macromol. Rapid Commun.* **1999**, *20*, 541.
(25) Beigzadeh, D.; Soares, J. B. P.; Duever, T. A. *Macromol. Symp.* **2001**, *173*, 179.
(26) Przybyla, C.; Fink, G. *Acta Polym.* **1999**, *50*, 77.
(27) Lieber, S.; Brintzinger, H.-H. *Macromolecules* **2000**, *33*, 9192.
(28) Chien, J. C. W.; Iwanoto, Y.; Rausch, M. D. *J. Polym. Sci., Part A: Polym. Chem.* **1999**, *37*, 2439.
(29) Chien, J. C. W.; Iwanoto, Y.; Rausch, M. D.; Wedler, W.; Winter, H. H. *Macromolecules* **1997**, *30*, 3447.
(30) Bruaseth, I. Ph.D. Thesis, Norwegian University of Science and Technology, Trondheim, 2003.
(31) Bruaseth, I.; Rytter, E. *Macromolecules* **2003**, *36*, 3026.
(32) Bruaseth, I.; Rytter, E. *Macromol. Symp.* **2004**, *213*, 69.
(33) Przybyla, C.; Fink, G. *Acta Polym.* **1999**, *50*, 77.
(34) Arrowsmith, D.; Kaminsky, W.; Schauwienold, A.-M.; Weingarten, U. *J. Mol. Catal. A: Chem.* **2000**, *160*, 97.
(35) Fan, W.; Waymouth, R. M. *Macromolecules* **2001**, *34*, 8619.
(36) *Landolt-Börnstein*, 6th ed.; Springer: Berlin, 1976; Part 4, Vol. C2, pp 126−129.
(37) Randall, J. C. *J. Macromol. Sci., Rev. Macromol. Chem. Phys.* **1989**, *C29*, 201.
(38) Scholte, T. G.; Meijerink, N. L. J.; Schoffeleers, H. M.; Brands, A. M. G. *J. Appl. Polym. Sci.* **1984**, *29*, 3763.
(39) Karssenberg, F. G.; Mathot, V. B. F.; Zwartkruis, T. J. G. *J. Polym. Sci. Part B: Polym. Phys.*, in press.
(40) Karssenberg, F. G.; Piel, C.; Hopf, A.; Mathot, V. B. F.; Kaminsky, W. *J. Polym. Sci. Part B: Polym. Phys.*, in press.
(41) Karssenberg, F. G.; Piel, C.; Hopf, A.; Mathot, V. B. F.; Kaminsky, W. *Macromol. Theory Simul.* **2005**, *14*, 295.
(42) Koivumäki, J.; Fink, G.; Seppälä, J. V. *Macromolecules* **1994**, *27*, 6254.
(43) Hu, W.; Karssenberg, F. G.; Mathot, V. B. F. *Polymer*, in press.

MA0505732